Available online at www.CivileJournal.org

Civil Engineering Journal

(E-ISSN: 2476-3055; ISSN: 2676-6957)

Vol. 10, No. 09, September, 2024

Comparative Study of UPV and IE Results on Concrete Cores from Existing Structures

Vassilis G. Siorikis [1, 2*], Constantinos P. Antonopoulos [1], George D. Hatzigeorgiou [2], Panagiotis Pelekis [3]

[1] *School of Pedagogical and Technological Education, Hellenic Open University, 14121 Athens, Greece.*

[2] *School of Science and Technology, Hellenic Open University, 14121 Athens, Greece.*

[3] *Department of Civil Engineering, University of Patras, Greece.*

Received 13 June 2024; Revised 19 August 2024; Accepted 27 August 2024; Published 01 September 2024

Abstract

Dynamic non-destructive methods (NDT) are particularly attractive owing to their time and cost efficiency when compared to conventional uniaxial compressive strength tests. However, the results of these methods are highly scattered; therefore, they are primarily used for qualitative material characterization. One of the most important NDT results is the calculation of the dynamic Young's modulus, which is associated to the uniaxial compressive strength (UCS) of concrete. The ultrasonic pulse velocity (UPV) is the most commonly used NDT. The limitation of this method is that it directly depends on knowledge of the Poisson's ratio, and an assumption of its value must be made. This assumption results in highly scattered results. In contrast, the impact echo method (IE) can result in a dynamic Young's modulus calculation without knowing the Poisson's ratio. The limitation of this method is that it is dependent on the specimen's slenderness, which in turn depends on the Poisson's ratio. This study investigates the IE method's applicability to short cylinders. A comparison of the UPV and IE methods is made, and the error in the dynamic Young's modulus value derived by assuming Poisson's ratio value in the UPV method is calculated. The authors conducted a numerical analysis and recently proposed the use of a shape correction factor (SCF) to apply the IE results for short cylinders, considering the influence of the slenderness (L/D) of the samples. For the first time worldwide, an extensive experimental study on 232 concrete samples with L/D ≈ 1.0 confirmed the wide spread of UPV test results and showed that it can lead to an error on Young's Modulus determination by up to 50% owing to the adoption of an arbitrary Poisson's ratio value. In contrast, using the SCF yields IE results with a ±2% error. A new methodology, ultrasonic pulse impact echo synergy (UPIES), is proposed by performing both UPV and IE tests on the specimens and using the SCF. The Poisson's ratio and, consequently, the Young's modulus can be accurately determined.

Keywords: Impact-Echo; Ultrasonic Pulse Velocity; Finite Element Method; Dynamic Poisson's Ratio; Dynamic Young's Modulus; Non-Destructive Testing; Acoustic Resonance.

1. Introduction

Engineers frequently have to perform tests on both old and new structures. The primary uses for new structures are most likely for material or construction quality control. The examination of existing structures is typically used to assess their structural integrity or adequacy. The tests available for this purpose range from completely non-destructive tests, such as ultrasonic pulse velocity (UPV) and rebound hammer tests, which do not cause any damage to the concrete, to partially destructive tests, such as the uniaxial compressive strength test (UCS), which requires the structure's surface

* Corresponding author: vsiorikis@aspete.gr

http://dx.doi.org/10.28991/CEJ-2024-010-09-03

to be repaired following the test. Non-destructive (NDT) and partially destructive tests can assess a wide range of properties, including fundamental parameters such as density, Young's modulus, and compressive strength, as well as surface hardness, absorption, steel reinforcement position, size, and distance from the surface. In some cases, gaps and detachments can be used to assess a construction's quality and structural integrity. Ideally, these tests should be performed without causing damage to the concrete; however, the only reliable method is UCS on concrete cores drilled from structures. The drawback of using only destructive tests, that is, core sampling for compression tests, is that the restoration cost is high; therefore, on a big structure, only a limited number of tests may be conducted; consequently, this can be misleading on a large scale. Therefore, NDT methods such as UPV and impact echo (IE) are increasingly being used worldwide.

The primary advantage of NDT is that it is both cost- and time-efficient. The integrity of a structure is evaluated by calculating the compressive strength of concrete using a well-known theoretical basis and user-friendly equipment. To calculate the compressive strength, the Young's modulus must be calculated first, and the Poisson's ratio must be known. However, the results of NDT methods must be evaluated using destructive tests, which both engineers and structural owners prefer to limit to a minimum. To reduce the number of destructive tests, the reliability of NDT results must be increased.

1.1. Ultrasonic Pulse Velocity (UPV) – ASTM C597-22

The most popular NDT method is the UPV method. An electroacoustical transducer in contact with one surface of the tested concrete produces pulses of longitudinal stress waves. After traversing the concrete, the pulses are received and converted into electrical energy by a second transducer located at a distance L from the transmitting transducer. The transit time T is measured electronically. The pulse velocity V is calculated by dividing L by T [1]. The primary result of this method is the dynamic Young's modulus. The correlation between the dynamic Young's modulus and UPV is shown in Equation 1 [2]. This correlation is not unambiguous but depends on the type of concrete, and the Poisson's ratio must be assumed [3].

$$E_d = \frac{\rho \times {V_p}^2 \times (1+\nu) \times (1-2\nu)}{1-\nu} \tag{1}$$

where ρ denotes mass density of the material, V_p denotes ultrasonic pulse velocity, and ν denotes Poisson's ratio.

In addition, using empirical equations, the UPV can be correlated with the concrete's compressive strength. Several studies have proposed different curves for obtaining this correlation [2–11]. However, the obtained correlation results are scattered, as shown in Figure 1, because of the influence of different factors such as the type of aggregate used and/or proportions, original water/cement ratio, curing conditions, level of compaction, and moisture content, where each curve is used to predict the strength of a specific concrete mix [4, 12]. However, the main issue is the arbitrary assumption of Poisson's ratio for the calculation of the dynamic Young's modulus, which results in scattered results and uncertainties.

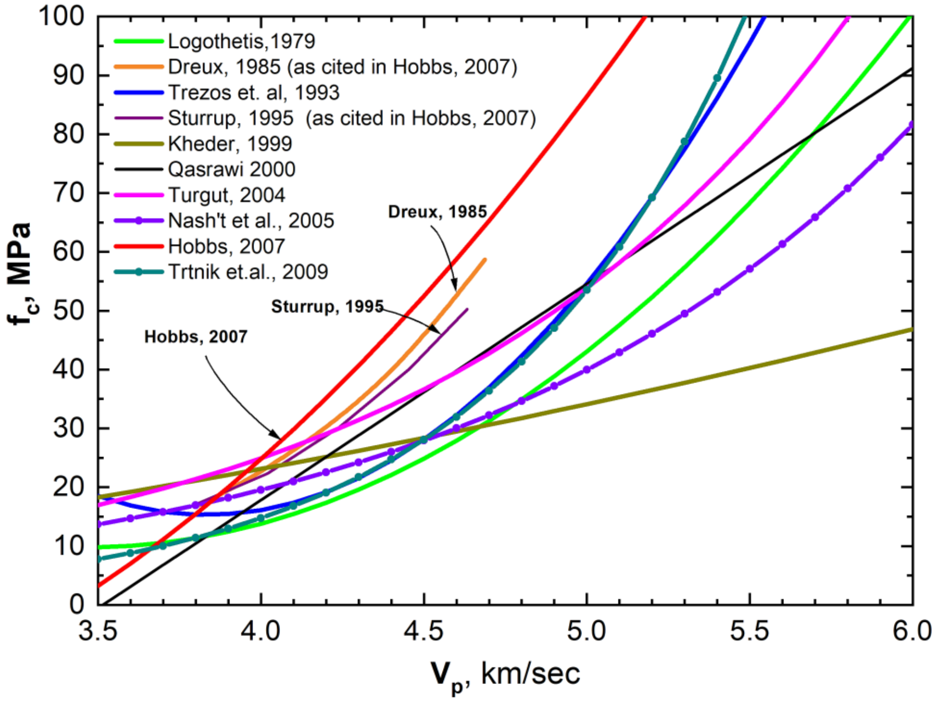

Figure 1. Empirical correlations of concrete compressive strength, f_c, versus V_p

ASTM Standard C-597 recommends the longitudinal resonance method in Test Method C 215, also known as the Impact Echo method, for determining the dynamic modulus of elasticity of test specimens obtained from field concrete, because the Poisson's ratio does not have to be known [1].

1.2. Impact-Echo Method (IE)

IE is another NDT method that is primarily used on concrete. The fundamental concept was developed by Sansalone and Carino in 1983 at the National Institute of Standards and Technology (NIST), where they conducted a long-term research program to provide a technical foundation for test methods for evaluating the concrete's in-place characteristics. The method was optimized by Professor Sansalone at Cornell University. This is a dynamic method based on an element's response to resonance. There are various applications, such as measuring the thickness of plates [13–17] and cylinders [9–10]and detecting defects, cracks, and cavities [16, 17]. When a material's dimensions are known, this method can be used to determine its dynamic properties using an inverse procedure [18].

The IE method involves impacting a supported specimen with a small object (usually a metallic sphere), measuring the specimen's response with a lightweight accelerometer with a sufficiently high frequency range, and recording the surface motion as a digital waveform in the time domain. These waveforms are converted to the frequency domain using the well-known fast Fourier transform (FFT) algorithm. The peaks obtained from the spectrum can be used to evaluate the structural integrity and the dynamic properties of materials, as well as to estimate the wave velocity [19]. One of the challenges with this method is correctly identifying the peaks that represent the resonant frequency. Malone et al. (2023) used a multi-impact nonlinear analysis to identify fundamental IE frequencies, while Pandum et al. (2024) used AI and deep learning algorithms to address this issue [20, 21].

When a solid's surface is subjected to mechanical impact, three transient voltage waves are produced: longitudinal waves (P-waves), shear waves (S-waves), and Rayleigh waves. The computation of these waves' propagation velocity in thin, finite-length bars forms the fundamental basis of the IE approach. After excitation, the specimen's free oscillation's resonance frequency is used to compute the propagation velocity as shown in Equation 2:

$$\mathbf{V_c = f \cdot 2L} \tag{2}$$

where V_c denotes wave propagation velocity in a rod with ratio L/D> 5; f denotes fundamental frequency of the first harmonic; L denotes specimen's length; and D denotes diameter of the specimen [22]. The Young's modulus is directly related to the rod velocity V_c through the following relation:

$$\mathbf{E_d = \rho \cdot V_c^2} \tag{3}$$

where ρ denotes mass density of the material [23].

From the above equation, it appears that it is possible to calculate the dynamic Young's modulus without knowing the value of Poisson's ratio, in contrast to Equation 1. The main drawback of the IE method for calculating rod velocity V_c is that the measured resonant frequency dependent on the slenderness ratio L/D. The frequency must be corrected using SCF which in turn depends on Poisson's ratio [12].

According to ASTM Standard C215, 2003, several studies use the fundamental resonant frequency of both prismatic and cylindrical concrete specimens. The dynamic modulus of the cylindrical specimens derives from the following equation:

$$\mathbf{E_d = 5,093 \frac{L}{D^2} \cdot M \cdot f^2} \tag{4}$$

where M denotes mass; f denotes fundamental longitudinal frequency; L denotes specimen's length, and D denotes specimen's diameter.

However, the ASTM Standard does not propose a correction for the longitudinal frequencies, while there are also limitations on specimens' dimensional ratio. Best results are obtained when this ratio is between three and five, with a minimum ratio of two. This is because when the lateral dimensions are not five or six times larger than the dimensions parallel to the impact, other vibration modes can interfere with the resonant frequency [24, 25]

Love (1944) in his treatise on the mathematical theory of elasticity used the following correction method:

$$\frac{f_{infinite}}{f_m} = \frac{1}{1-\left(\frac{L}{D}\right)^{-2}\frac{\pi^2}{16}\nu^2} \tag{5}$$

where $f_{infinite}$ denotes the theoretical resonant frequency, f_m denotes the measured frequency, L denotes specimen's length, D denotes specimen's diameter, and ν denotes Poisson's ratio [26].

Subramaniam et al. (2000) showed that Young's modulus can be determined using Poisson's ratio and the first resonant frequency as follows:

$$E_d = 2\,(1+\nu)\,\rho\,\left(\frac{2\pi\, f_1 R_0}{{f_n}^1}\right)^2 \tag{6}$$

$${f_n}^1 = A_2\,(\nu)^2 + B_2(\nu) + C_2 \tag{7}$$

where f_1 denotes measured frequency, R_0 denotes cylinder's radius, ρ denotes material's density A_2, B_2 and C_2 coefficients depend on the L/D ratio [27].

Most studies have investigated the influence of slenderness L/D> 2.0. However, it is more useful to obtain results for specimens with L/D=1 and approximately, because this is the typical size of concrete cores drilled from existing structures. The results of the IE implementation on small, short cylinders differ fundamentally from those on large, long cylinders and cannot be described using the existing calculation formulas. To consider the influence of L/D, the measured frequencies must be corrected. The need for correction of the IE implementation was also identified by Yao et al. (2022) who proposed Equation 8 for frequency correction [28].

$$f_{ie} = [(0.58L^{-1{,}01})\cdot D - 0.060]\;\frac{0.92\cdot C_P}{2D} \tag{8}$$

where f_{ie} denotes frequency correction, L denotes specimen's length, D denotes specimen's diameter, and C_p denotes wave propagation velocity.

Equation 9 was proposed in the present study for calculating SCF, y, based on an extensive numerical simulation of the IE method over a wide range of L/D from 0.7 to 5.0 [12, 29].

$$y = y_o + A_1 e^{-x/t_1} + A_2 e^{-x/t_2} \tag{9}$$

where y denotes shape's correction factor, x denotes L/D ratio, and y_o, A_1, A_2, t_1, t_2 are coefficients that depend on Poisson's ratio. The SCF is not only influenced by L/D, but also depends directly on the Poisson's ratio, as verified by Wang et al., 2012 and Authors, 2022 [30, 31].

It is clear that knowledge of Poisson's ratio is crucial. To overcome this limitation, we propose using two NDT methods simultaneously rather than just the UPV or IE. Therefore, this study presents a novel methodology for accurately calculating the Poisson's ratio, called ultrasonic pulse impact echo synergy (UPIES). First, the experimental setup is explained. Three tests–UPV, IE, and UCS–were conducted on concrete cores from existing structures and then integrated into the Poisson's ratio calculation. Subsequently, a numerical simulation setup leading to the proposed SCF is presented. On this basis, this study presents an experimental confirmation of UVP scattering and calculates the error of using this method as a standalone method. Following the simultaneous use of UPV and IE, the Poisson's ratio is now known, and the error is calculated using the proposed SCF from the numerical analysis. Finally, a comparison of the two methods is performed, and a new methodology and implementation are proposed before drawing conclusions.

2. Experimental Study of UPV and IE Methods

To confirm the uncertainty associated with the Poisson's ratio, an extensive experimental investigation was conducted for the first time worldwide, with 232 concrete cores drilled from pre-existing structures (buildings and bridges) and tested using UPV and IE before being subjected to uniaxial compression testing. The buildings were constructed between 1960 and 1990 with a compressive strength between $C_{12/15}$ and $C_{20/25}$, according to European Standard EN 206, and an aggregate grain size of 25–30 mm. Four bridges were sampled for this study. Three were constructed using conventional concrete with a maximum grain size of 30–35 mm between 1960 and 1970, and one with prestressed concrete and natural aggregates with a maximum grain size of 25 mm in 1970. The concrete for all four bridges was categorized as $C_{20/25}$.

The samples' height and diameter were measured after coring but before using any method, and the L/D ratio was calculated. Figure 2 shows the dimensions of the number of samples in the histogram view. The diameter of 95% of the cores varied between 9.5 and 10.5 cm, resulting in L/D= 1.

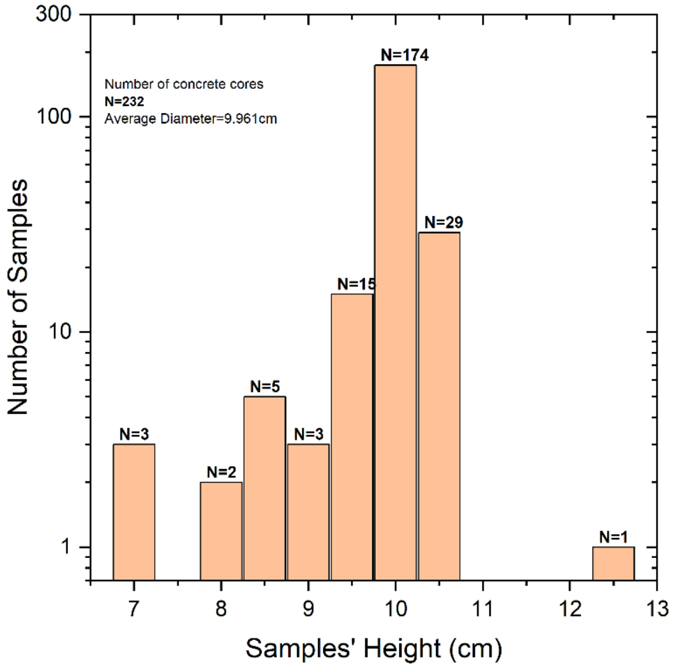

Figure 2. Results of samples' height

2.1. UPV Test

A Proceq Tico apparatus was used for the UPV test, as shown in Figure 3. The transducers were typical 54 kHz P-wave transducers used in UPV tests on concrete, and the ultrasonic pulse velocity V_p was measured.

Figure 3. UPV apparatus testing concrete specimen

2.2. IE Test

The IE method was implemented using a Kistler's accelerometer with a measuring range of ±50 g, sensitivity of 100.3 mV/g, and weight of 10.6 grams. The signals were analyzed and recorded using an Agilent 35670A Digital Signal Analyzer (DSA) as observed in Figure 4. Using the resulting spectra and FFT, the resonant frequencies were identified, and the rod velocity, V_c, was measured.

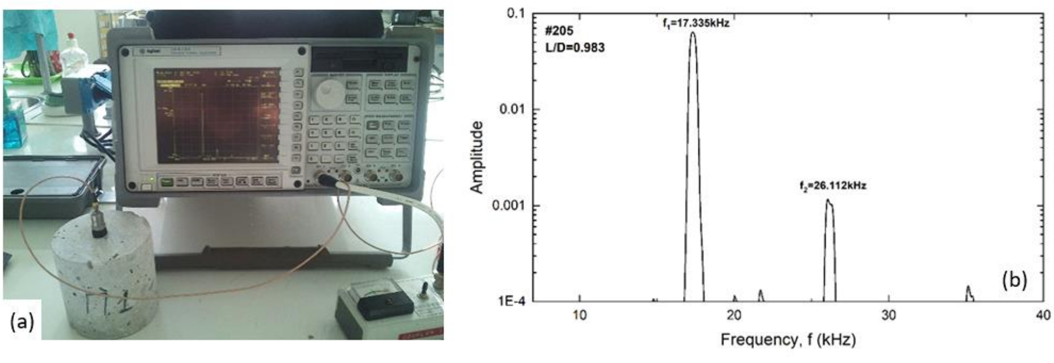

Figure 4. (a) IE apparatus testing concrete sample and (b) Frequency Spectrum

2.3. Uniaxial Compression Test

Finally, the samples were tested under uniaxial compression with an Impact CS7156 Compression machine with a load cell capacity of 2000 kN, and the Greek Bulletin E7 correction was used to compute the concrete's compressive strength. This correction is appropriate for determining the strength class of existing structures [32].

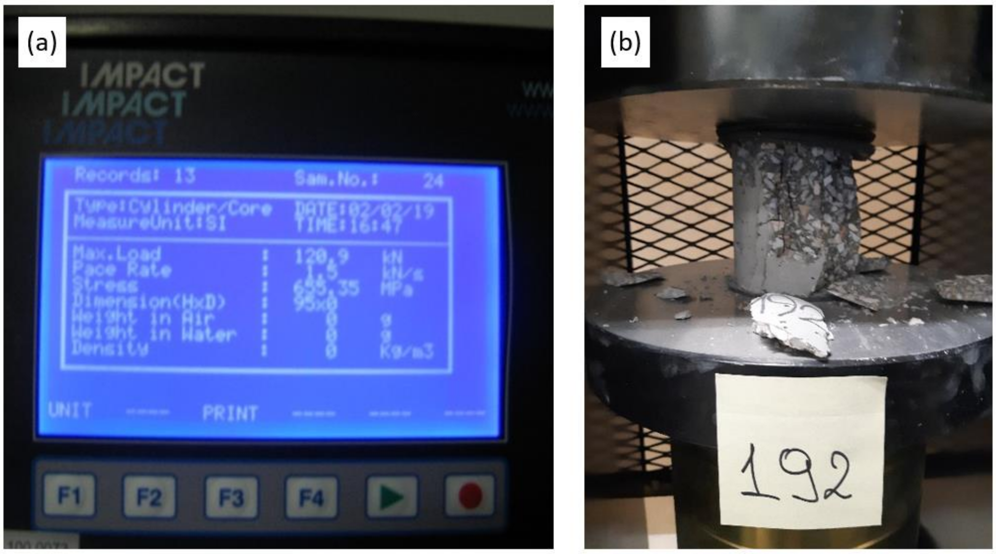

Figure 5. (a) Uniaxial compression machine (b) Concrete specimen after testing

2.4. Poisson's Ratio Calculation

From the results of the simultaneous UPV and IE tests, Poisson's ratio can be directly determined through Equation 10 using Equations 3, 11, and 12.

$$\nu = \frac{E_d - M + S}{4 \cdot M} \tag{10}$$

$$M = \rho \cdot {V_p}^2 \tag{11}$$

$$S = \pm\sqrt{{E_d}^2 + 9M^2 - 10E_dM} \tag{12}$$

where M denotes P-wave Modulus, V_p denotes the velocity of a P-wave, and ρ denotes the density of the material through which the wave is propagating.

3. Numerical Simulation of IE Method – Shape Correction Factor

A total of 72 simulations were conducted to evaluate how the specimen shape affected the determination of Poisson's ratio. For the numerical simulation of the IE test, the Plaxis 2D finite element software was used, which allows for the creation of an axisymmetric model around a central axis, as shown in Figure 6(a). This study used 15-node finite elements to create models with the following parameters: (a) L/D= 0.7, 0.8, 1.0, 1.2, 1.4, 1.6, 1.8, 2.0, 2.5, 3.0, 4.0, and 5.0; and (b) Poisson's ratio, v= 0.20, 0.25, 0.30, 0.36, 0.40, and 0.45. In all simulations, the diameter was constant and equal to 0.1 m. The rationale for selecting the data set was based on a very wide range of Poisson's ratio values, that can represent not only concrete but all the materials, and a wide range of slenderness's values, but not smaller than 0.7, as the record of the wave propagation becomes very complex owing to reflections, and not greater than 5.0, as the cylinder can be considered as an infinite thin rod. As previously stated, most of the studies investigate the influence of slenderness L/D> 2.0. The goal of the simulation was to investigate the results close to smaller slenderness, so the parameter of L/D was changed by 0.2 increments between 0.8–2.0, while for larger slenderness, where the theory already backs up the results, the choice of increments was less sensitive. The entire range of Poisson's ratios was investigated in increments of 0.05. The sensitivity analysis method is one-at-a-time (OAT), where only one input at a time varies while others remain constant to observe the difference in frequency output.

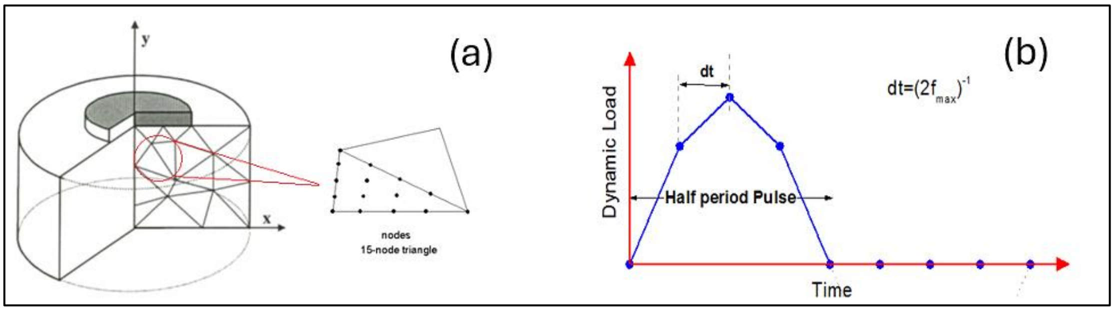

Figure 6. (a) Axisymmetric model using 15-node FE and (b) Excitation's harmonic pulse

To reduce the computational time, only half of the specimens' circular cross-section were modeled; therefore, the horizontal displacement at the nodes along the vertical plane of symmetry had to be constrained.

Plaxis provides an automated mesh construction algorithm that allows the user to change the mesh fineness and coarseness. The total number of elements and their sizes are determined using the maximum desired frequency. Specifically, the maximum frequency, f_{max}, was determined to be five times the expected frequency of the first resonant frequency, which is sufficiently broad to capture the desired resonance while maintaining computational efficiency. The dynamic analysis time interval, Δt, was derived directly from f_{max} as shown below:

$$\Delta t = \frac{1}{2 \cdot f_{max}} \tag{13}$$

and were selected such that the wave would not travel a distance larger than the smallest size of the finite element during a step.

The excitation was modeled using a half-sine pulse, as shown in Figure 6(b). The duration of excitation was determined as half the value of the sine period divided by the selected number of time steps of the excitation phase. The pulse frequency was selected each time such that its value was close to that of the first resonant frequency. The first dominant resonant frequency was identified using the FFT spectra of the time history. A free oscillation spectrum calculation example is presented in Figure 7, where the first and second prominent resonant normalized frequencies for L/D = 1.0 and 5.0 are indicated in black and red namely.

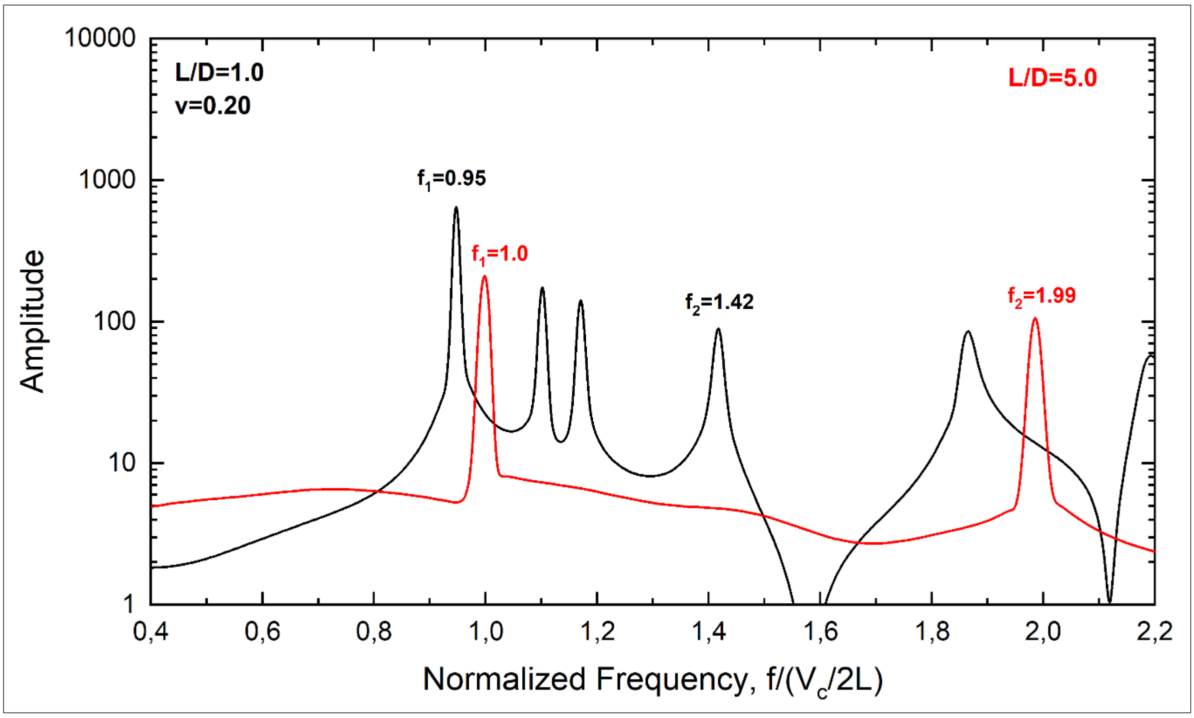

Figure 7. Normalized frequency spectrum with the values of the first dominant resonant frequency marked for two values of slenderness

For a known V_p, the theoretical wave propagation velocity V_c was derived using Equations 1 and 3, and the theoretical first resonant frequency of the wave propagation is calculated using Equation 2. Equation 14 considers SCF equal to the ratio of the theoretical to finite element method (FEM), which is the first dominant frequency.

$$SCF = \frac{f_{Theoretical}}{f_{FEM}} \tag{14}$$

When the above SCF is applied to all the Poisson's ratio values, it yields Equation 9, which is then incorporated into Equation 2, to correct the calculation of the rod velocity as follows:

$$V_c = (f_m \cdot SCF) \cdot 2L \tag{15}$$

where f_m denotes the measured resonant frequency Equation 9.

4. Results and Discussion

4.1. FEM results – Shape Correction Factor

Table 1 shows the FEM analysis results for a given velocity V_p and Poisson's ratio value for 12 different slenderness values, with the calculated theoretical first resonant frequency in the second column. The third column contains the first resonant frequency derived from the FEM analysis, and the fourth column contains the SCF calculated from Equation 14. Figure 8 shows the SCF versus slenderness L/D for six Poisson's ratio values.

Table 1. Results of FEM Analysis

L\D	$f_{1,\ Theroretical}$ (Hz)	$f_{1,FEM}$ (Hz)	SCF
5.0	189.7	189.7	1.0002
4.0	237.2	237.1	1.0003
3.0	316.2	315.8	1.0014
2.5	379.5	378.5	1.0026
2.0	474.3	471.7	1.0056
1.8	527.0	523.0	1.0077
1.6	592.9	586.0	1.0118
1.4	677.6	665.0	1.0190
1.2	790.6	768.0	1.0294
1.0	948.7	899.0	1.0553
0.8	1185.9	1050.0	1.1294
0.7	1355.3	1122.0	1.2079

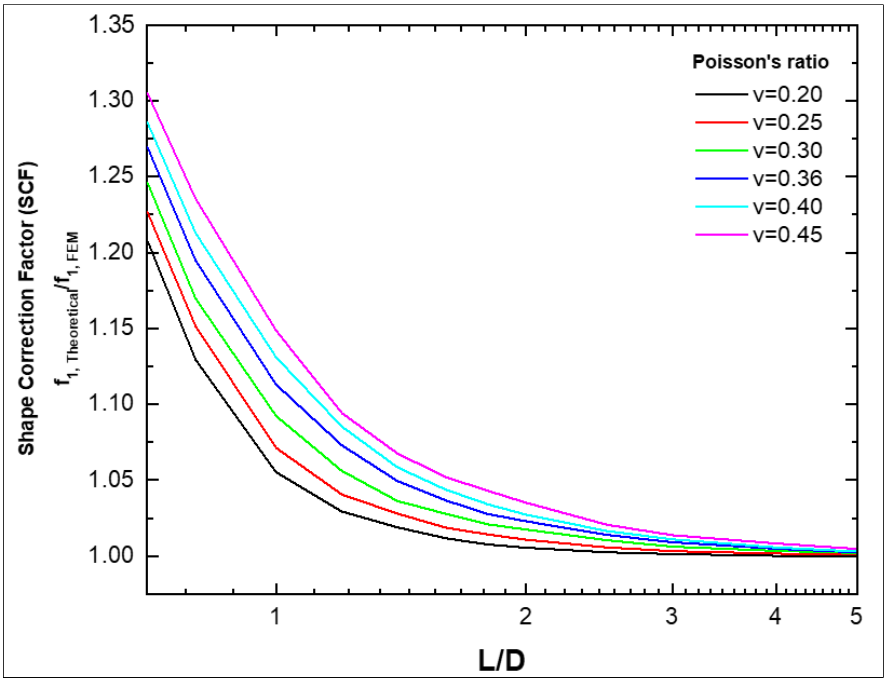

Figure 8. Shape Correction Factor versus slenderness L/D for six Poisson's ratio values diagrams

Evidently, a larger adjustment is required when the slenderness decreases. This demonstrates why SCF is crucial for short cylinders. The adjustment is substantial, and assuming a value for the Poisson's ratio can result in significant inaccuracy, particularly near L/D=1, which is the normal size of concrete cores.

Figure 9 shows a comparison between the SCF of the present study and the proposed CF of Love, as expressed by Equation 5. The two CFs are similar, although the proposed SCF provides a larger correction. For L/D=1, the variation in the two CF's was only 2.8%, with an average Poisson's ratio of v= 0.32.

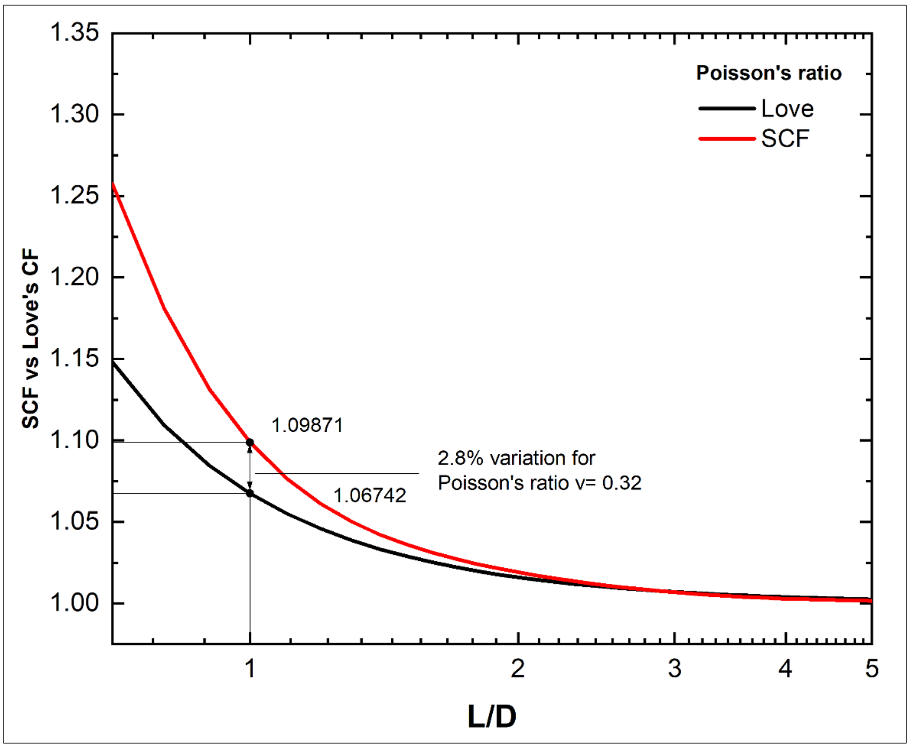

Figure 9. SCF comparison to Love's CF for an average values of Poisson's ratio v=0.32

4.2. Experimental Confirmation of UPV Scatter – Error Calculation

After testing the 232 cores and calculating Poisson's ratio using Equation 10, statistical analysis of the results reveals that Poisson's ratio varies from 0.25 to 0.44, with an average value of $v = 0.32$. The histogram in Figure 10 shows the samples' probability mass function versus the dynamic Poisson's ratio. For the lower 10% of the samples, the Poisson's ratio is $v < 0.288$, while for the higher 10% of the samples, $v > 0.356$, as shown in the cumulative distribution function in Figure 11.

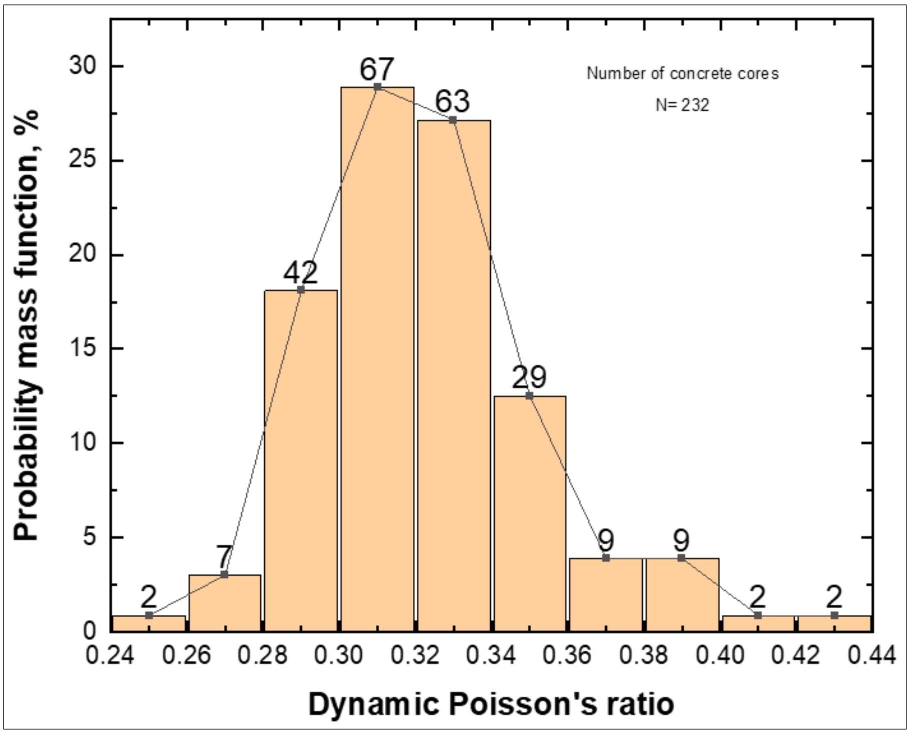

Figure 10. Distribution of dynamic Poisson's ratio of the tested concrete samples

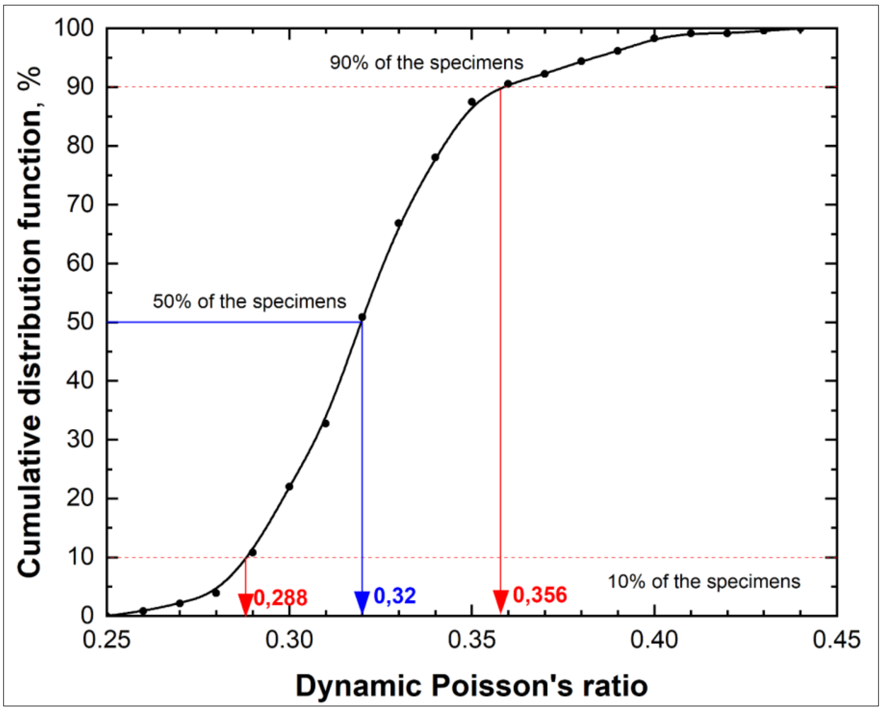

Figure 11. Cumulative distribution function of 232 tested concrete cores

The measured longitudinal wave velocities are compared to the compressive strength of each core, as shown in Figure 12, and the scatter of the UPV method is confirmed. The blue dots represent the scattered values of V_p caused by the Poisson's ratio variation, while the red dots represent the values of V_c obtained from IE, which are significantly less scattered. Figure 13 shows that the two methods, UPV and IE, are equivalent, particularly for a narrower range of Poisson's ratio, v= 0.25–0.30.

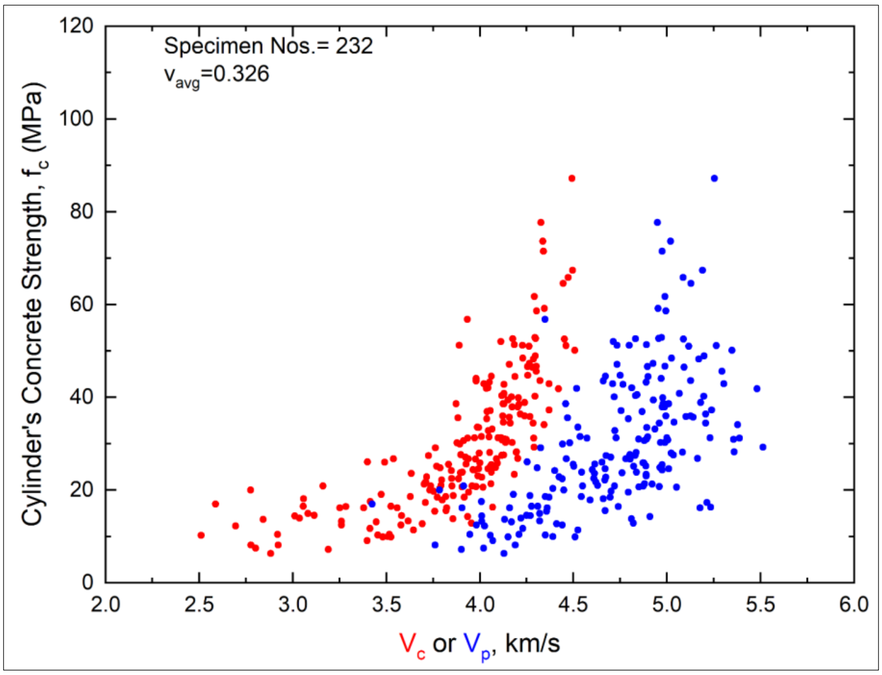

Figure 12. Compressive strength vs velocity Vc and $\mathbf{V_p}$

If we normalize the quantity $(1+\nu)*(1-2\nu)/\,(1-\nu)$ of Equation 1, which serves as a correction factor for E_d calculation, for Poisson's ratio values from v= 0.24–0.44, the curves of Figure 14 derive. According to Equation 16, the error of the dynamic Poisson's ratio v_d and, by extension, the E_d estimation when an arbitrary value of Poisson's ratio is adopted can be calculated, as depicted in Figure 14.

$$E\% = \frac{v_{d,Real} - v_{d,assumed}}{v_{d,Real}} \tag{16}$$

where $v_{d,Real}$ denotes the real Poisson's ratio and $v_{d,assumed}$ denotes the assumed Poisson's ratio.

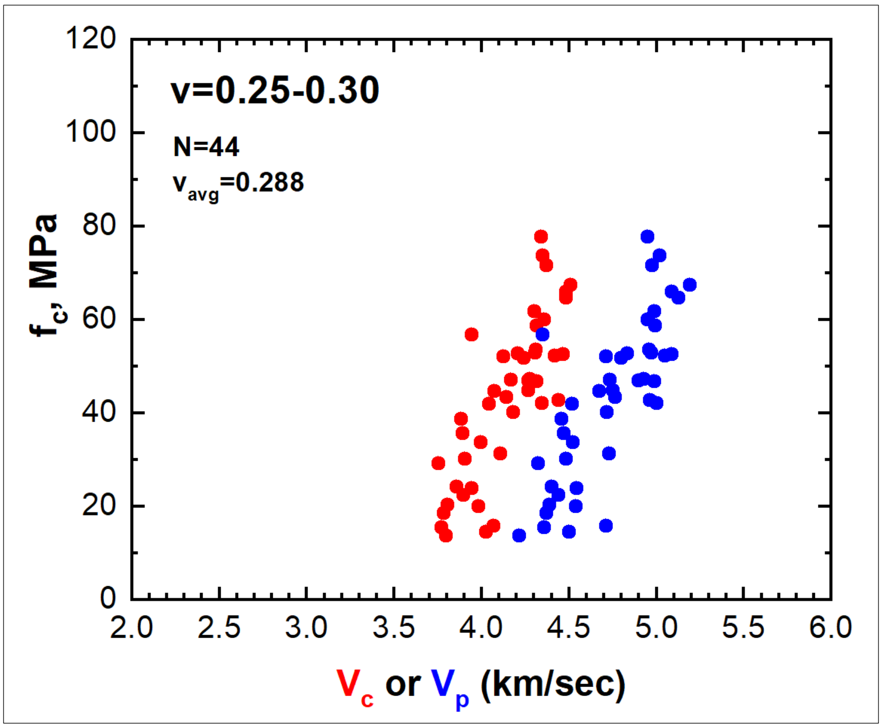

Figure 13. Compressive strength vs velocities Vc and Vp for a narrow range of Poisson's ratio

In particular, when the average value of Poisson's ratio, v= 0.32, is assumed, the associated error in estimating E_d can be significant, varying from 8.5% (overestimation) if the true Poisson's ratio is 0.288 to 15.5% (underestimation) if the true Poisson's ratio is 0.356, whereas for v= 0.40, this error can reach up to 50% underestimation.

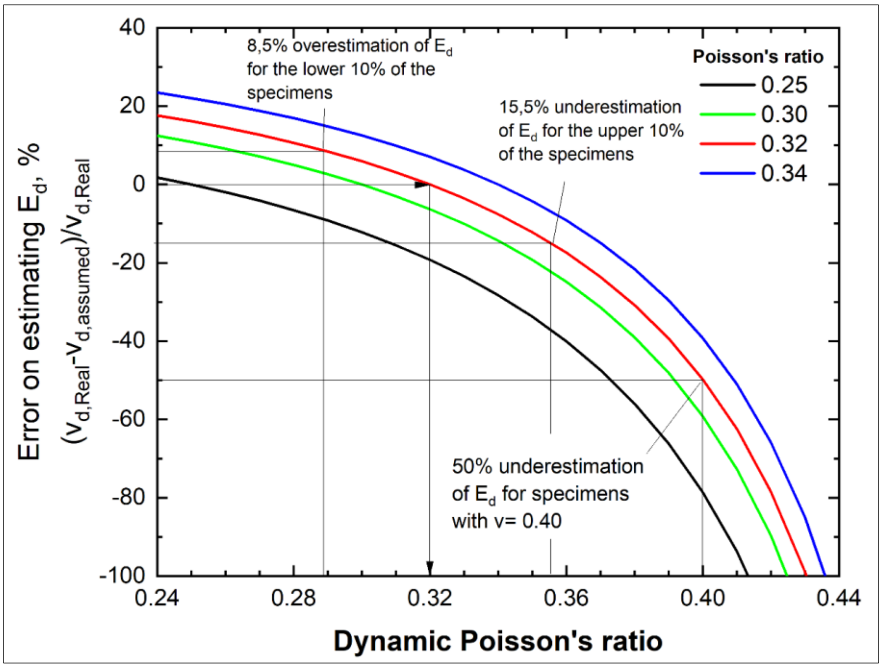

Figure 14. Error on E_d estimation associated with the selection of an arbitrary Poisson's ratio value

Consequently, the UPV is frequently regarded as unreliable for determining the dynamic Young's modulus and compressive strength of concrete and cannot be considered a safe standalone method.

4.3. Estimation of Young's modulus using the new methodology UPIES

However, testing with the IE and proposed SCF appears to be more accurate. Equation 9, with an average Poisson's ratio of v=0.32, can accurately estimate the dynamic Young's modulus. In Figure 15, the black solid curve represents the SCF for v= 0.32. The error is less than 2% for L/D= 2.0, but approximately 9.8% for L/D= 1.0 (v= 0.32 ± 0.0313).

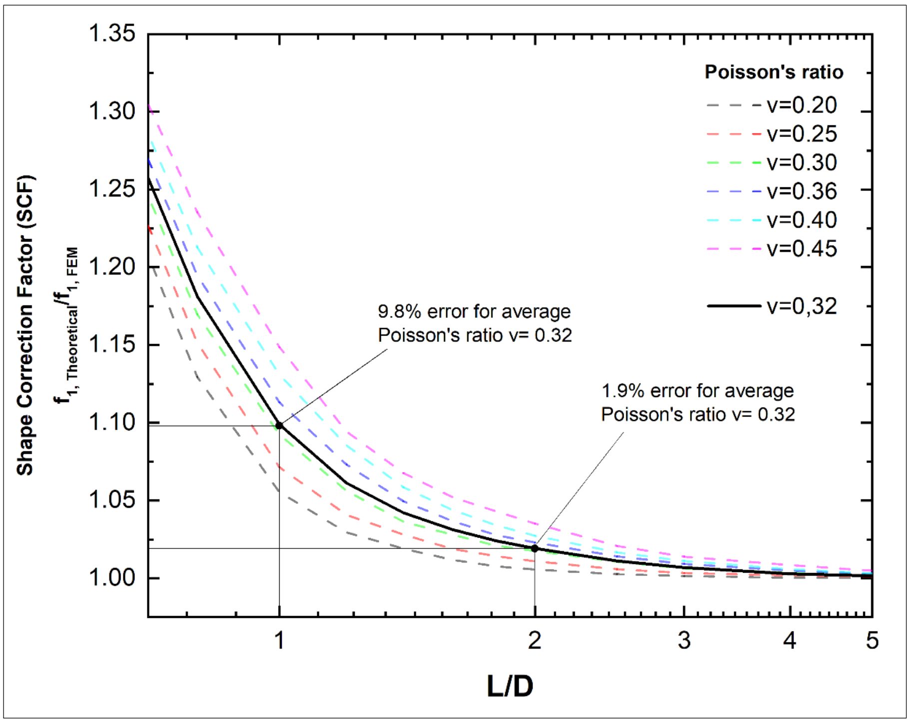

Figure 15. Shape Correction Factor versus slenderness L/D for six Poisson's ratio values diagrams, with the calculation error of the average Poisson's ratio for L/D= 1.0 and L/D= 2.0 marked

Figure 16 shows that for L/D= 1.0, which is the typical size of the concrete core taken from structures, the SCF varies between 1.05 and 1.15, resulting in a total error variation of 8.1% across the entire range of Poisson's ratios. This error decreases significantly when the range is narrowed down to the typical Poisson's ratio values of concrete. For Poisson's ratio values v= 0.20–0.25 the variation of the correction factor is only 1.5%, while for v= 0.25–0.30 and v= 0.30–0.35 the variation is 1.9%, as shown in Figure 17.

From Figure 14, we can draw the conclusion that it is not safe to use UPV as a standalone method; while, this is also supported if we compare the two methods, where it is evident that the proposed IE SCF surpasses the UPV CF owing to the significantly smaller potential error. The limitation of Poisson's ratio value knowledge can be eliminated by the simultaneous use of the IE and UPV tests and Equations 3 and 10, which result in the new proposed methodology.

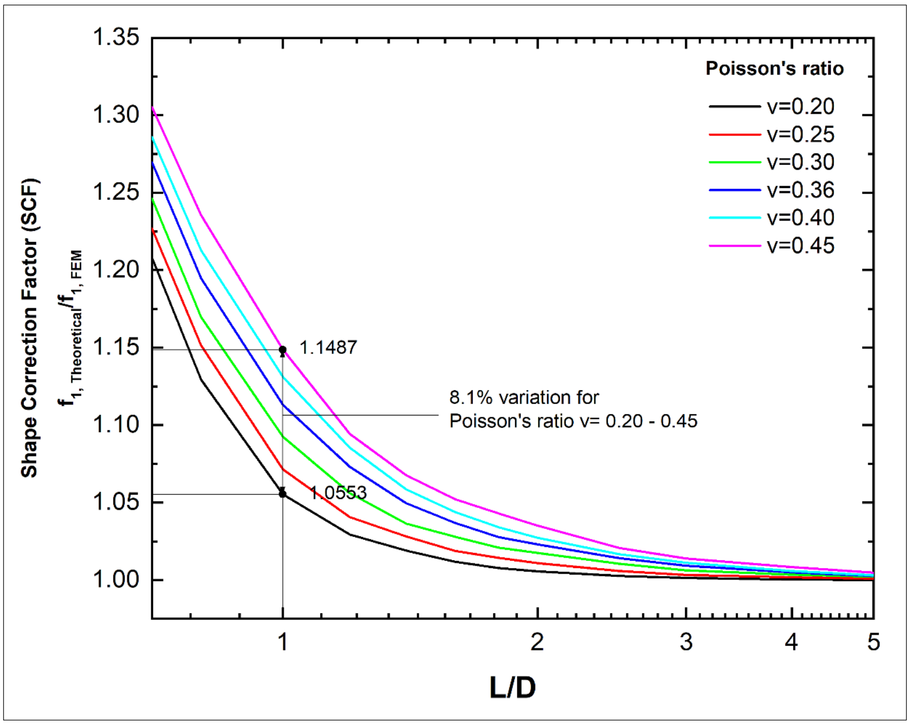

Figure 16. Shape Correction Factor versus slenderness L/D for six Poisson's ratio values diagram with the error variation marked

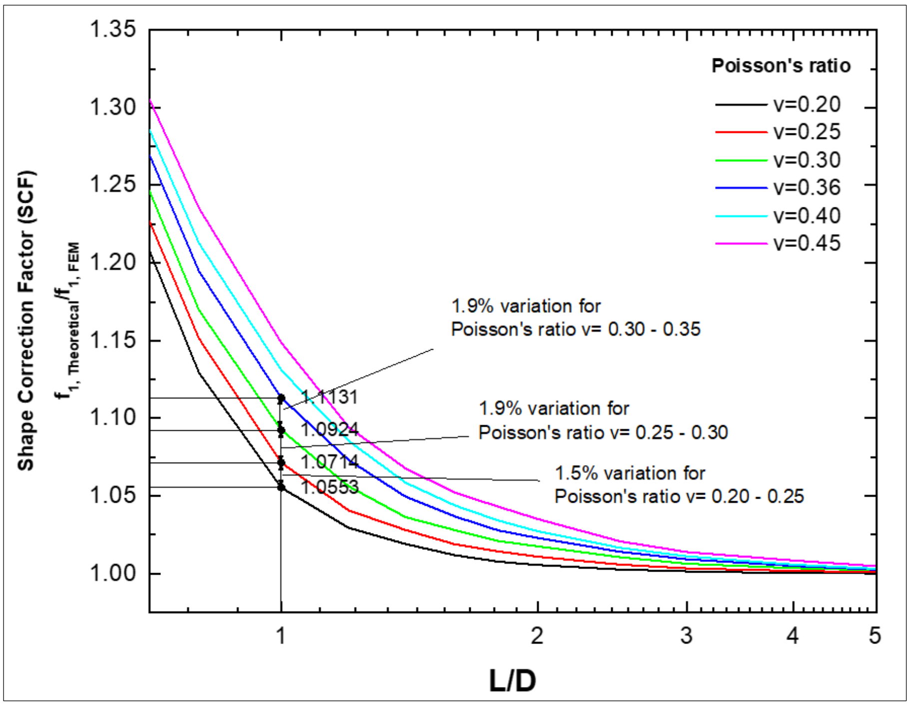

Figure 17. Shape Correction Factor versus slenderness L/D for six Poisson's ratio values diagram with the error variation for the typical dynamic Poisson's ratio on concrete marked

The new methodology is called UPIES and can be applied by following the steps shown in Figure 18 and visualized in Figure 19.

Step 1: Ultrasonic Pulse Velocity, Vp calculation: through UPV method application

↓

Step 2: First resonant frequency, fc calculation: through IE method application

↓

Step 3: Correction of the measured fc through the proposed SCF and fc,cor calculation

↓

Step 4: Thin rod velocity Vc calculation through the Equation 15

↓

Step 5: Constrained and Young Moudulus calculation through the Equations 3, 11

↓

Step 6: Poisson's ratio calculation through Equation 10

Figure 18. Flowchart illustrating the proposed procedure for determining Poisson's ratio value

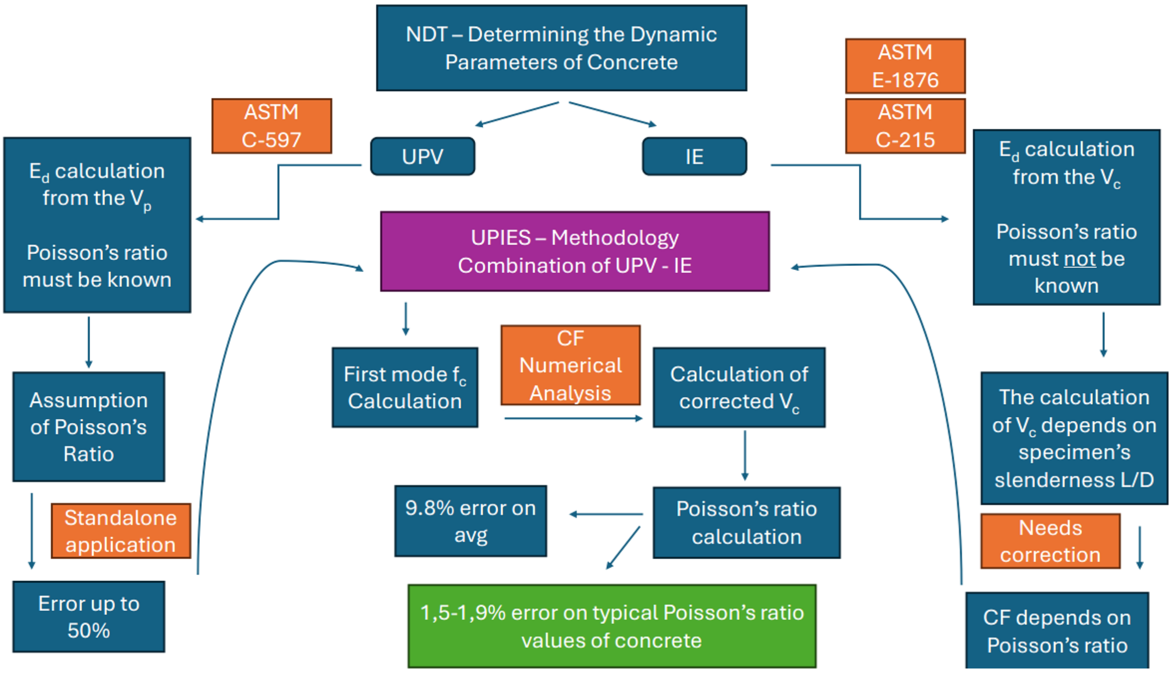

Figure 19. Flowchart of implementation of the UPIES - new methodology

5. Conclusion

NDT is crucial for civil engineers to assess the mechanical properties of concrete, such as the Poisson's ratio, Young's modulus, and compressive strength. However, NDT methods frequently have uncertainties that necessitate validation through destructive testing, which is expensive, time-consuming, and requires surface restoration. The primary objective of this field is to develop more reliable NDT methods that can eliminate the need for destructive testing. The UPV test is one of the most commonly used NDT methods for determining dynamic Young's modulus. However, this requires an assumed Poisson's ratio, which can result in significant errors. As an alternative, the IE method recommended by ASTM Standard C-597 does not require this assumption and potentially offers more accurate results.

This study includes the first experimental comparison of the UPV and IE methods on 232 concrete specimens worldwide, as well as a detailed numerical analysis of 72 specimens using the FEM. The results showed that using an arbitrary Poisson's ratio in UPV can result in an error margin ranging from -15.5 to +8.5%, and even up to 50% for higher Poisson's ratios. In contrast, the IE method exhibited lower variability. Using a SCF derived from FEM simulations, the error was found to be up to 9.8% for an average value of Poisson's ratio v= 0.32 over the entire range of Poisson's ratio, which is considerably smaller than the error derived from the UPV method. In a smaller, more reasonable range of Poisson's values is less than 2%. This procedure significantly reduced errors in the IE method, particularly for a typical concrete core size. Finally, a new methodology, UPIES, was proposed that combines the UPV and IE methods to provide more reliable determinations of the dynamic Poisson's ratio and Young's modulus, improving the accuracy of NDT in concrete evaluation.

6. Declarations

6.1. Author Contributions

Conceptualization, P.P. and V.G.S.; methodology, P.P.; software, P.P.; validation, P.P., K.P.A., and G.D.H.; formal analysis, P.P. and V.G.S.; investigation, P.P., V.G.S., and K.P.A.; resources, P.P. and K.P.A.; data curation, P.P., K.P.A., and V.G.S.; writing—original draft preparation, V.G.S.; writing—review and editing, P.P.; visualization, V.G.S. and P.P.; supervision, P.P.; project administration, P.P. and V.G.S.; funding acquisition, P.P. All the authors have read and agreed to the published version of the manuscript.

6.2. Data Availability Statement

The data presented in this study are available on request from the corresponding author.

6.3. Funding and Acknowledgements

This study has been financed by the University of Patras, department of Civil Engineering and the Greek School of Pedagogical and Technological Education through the operational program "Research strengthening in ASPETE"– Project 80154: "Determination of Compressive Strength and Other Mechanical Concrete Parameters by Sonic Resonance (Experimental and Numerical Investigation)". We would like to thank Editage (www.editage.com) for English language editing.

6.4. Conflicts of Interest

The authors declare no conflict of interest.

7. References

[1] ASTM C597. (2016). Standard Test Method for Pulse Velocity Through Concrete. American Society for Testing and Materials (ASTM), Pennsylvania, United States.

[2] Panzera, T. H., Christoforo, A. L., de Paiva Cota, F., Ribeiro Borges, P. H., & Bowen, C. R. (2011). Ultrasonic Pulse Velocity Evaluation of Cementitious Materials. Advances in Composite Materials - Analysis of Natural and Man-Made Materials. Intechopen, London, United Kingdom. doi:10.5772/17167.

[3] ASTM-E1876-22. (2000). Standard Test Method for Dynamic Young's Modulus, Shear Modulus, and Poisson's Ratio by Impulse Excitation of Vibration. American Society for Testing and Materials (ASTM), Pennsylvania, United States.

[4] Hobbs, B., & Tchoketch Kebir, M. (2007). Non-destructive testing techniques for the forensic engineering investigation of reinforced concrete buildings. Forensic Science International, 167(2–3), 167–172. doi:10.1016/j.forsciint.2006.06.065.

[5] Logothetis, L. (1979). A contribution to the in-situ assessment of concrete strength by means of combined non-destructive methods. Ph.D. Dissertation, National Technical University, Athens, Greece. doi:10.12681/eadd/2558. (in Greek)

[6] Trezos, K., Papakyriakopoulos, P., & Spanos, C. (1993). Calibration of the Rebound Hammer and Pulse Velocity Methods through in situ concrete cores and standard cube specimens. Technical Chamber of Greece, Agrinio, Greece.

[7] Turgut, P. (2004). Evaluation of the ultrasonic pulse velocity data coming on the field. Fourth International Conference on NDE in Relation to Structural Integrity for Nuclear and Pressurised Components, 573–578.

[8] Trtnik, G., Kavčič, F., & Turk, G. (2009). Prediction of concrete strength using ultrasonic pulse velocity and artificial neural networks. Ultrasonics, 49(1), 53–60. doi:10.1016/j.ultras.2008.05.001.

[9] Qasrawi, H. Y. (2000). Concrete strength by combined nondestructive methods simply and reliably predicted. Cement and Concrete Research, 30(5), 739–746. doi:10.1016/S0008-8846(00)00226-X.

[10] Kheder, G. F. (1999). Two stage procedure for assessment of in situ concrete strength using combined non-destructive testing. Materials and Structures/Materiaux et Constructions, 32(6), 410–417. doi:10.1007/bf02482712.

[11] Nash't, I. H., Saeed, H. A., & Sadoon, A. A. (2005). Finding an Unified Relationship between Crushing Strength of Concrete and Non-destructive Tests. 3rd MENDT - Middle East Nondestructive Testing Conference & Exhibition, 27-30 November, 7.

[12] Siorikis, V. G., Antonopoulos, C. P., Pelekis, P., Christovasili, K., & Hatzigeorgiou, G. D. (2020). Numerical and experimental evaluation of sonic resonance against ultrasonic pulse velocity and compression tests on concrete core samples. Vibroengineering Procedia, 30, 168–173. doi:10.21595/vp.2020.21328.

[13] Medina, R., & Bayón, A. (2010). Elastic constants of a plate from impact-echo resonance and Rayleigh wave velocity. Journal of Sound and Vibration, 329(11), 2114–2126. doi:10.1016/j.jsv.2009.12.026.

[14] Nieves, F. J., Gascón, F., & Bayón, A. (2000). Precise and direct determination of the elastic constants of a cylinder with a length equal to its diameter. Review of Scientific Instruments, 71(6), 2433–2439. doi:10.1063/1.1150632.

[15] Nieves, F. J., Gascón, F., & Bayón, A. (2003). Measurement of the dynamic elastic constants of short isotropic cylinders. Journal of Sound and Vibration, 265(5), 917–933. doi:10.1016/S0022-460X(02)01563-8.

[16] Sansalone, M. (1997). Impact-echo: The complete story. ACI Structural Journal, 94(6), 777–786. doi:10.14359/9737.

[17] Lee, K.-M., Kim, D.-S., & Kim, J.-S. (1997). Determination of dynamic Young's modulus of concrete at early ages by impact resonance test. KSCE Journal of Civil Engineering, 1(1), 11–18. doi:10.1007/bf02830459.

[18] ASTM C215. (2008). Standard Test Method for Fundamental Transverse, Longitudinal, and Torsional Resonant Frequencies of Concrete Specimens. American Society for Testing and Materials (ASTM), Pennsylvania, United States. doi:10.1520/C0215-14.2.

[19] Pandum, J., Hashimoto, K., Sugiyama, T., & Yodsudjai, W. (2024). Impact-Echo for Crack Detection in Concrete with Artificial Intelligence based on Supervised Deep Learning. e-Journal of Nondestructive Testing, 29(6), 1-12. doi:10.58286/29925.

[20] Malone, C., Sun, H., & Zhu, J. (2023). Nonlinear Impact-Echo Test for Quantitative Evaluation of ASR Damage in Concrete. Journal of Nondestructive Evaluation, 42(4), 93. doi:10.1007/s10921-023-01003-2.

[21] Schubert, F., & Köhler, B. (2008). Ten lectures on impact-echo. Journal of Nondestructive Evaluation, 27(1–3), 5–21. doi:10.1007/s10921-008-0036-2.

[22] Prakash, S. (1981). Soil Dynamics. McGraw-Hill, New York, United States.

[23] Dethof, F., & Keßler, S. (2024). Explaining impact echo geometry effects using modal analysis theory and numerical simulations. NDT and E International, 143. doi:10.1016/j.ndteint.2023.103035.

[24] ASTM C1383-15. (2022). Standard Test Method for Measuring the P-Wave Speed and the Thickness of Concrete Plates Using the Impact-Echo Method. American Society for Testing and Materials (ASTM), Pennsylvania, United States.

[25] LNG. F. (1920). A Treatise on the Mathematical Theory of Elasticity. Nature 105, 511–512. doi:10.1038/105511a0.

[26] Kolluru, S. V., Popovics, J. S., & Shah, S. P. (2000). Determining elastic properties of concrete using vibrational resonance frequencies of standard test cylinders. Cement, Concrete and Aggregates, 22(2), 81–89. doi:10.1520/cca10467j.

[27] Yao, F., Zhuang, J., & Abulikemu, A. (2022). Shape coefficient of impact-echo for small-size short cylinder/circular tube structures. Materialpruefung/Materials Testing, 64(4), 574–583. doi:10.1515/mt-2021-2043.

[28] Siorikis, V. G., Antonopoulos, C. P., Pelekis P., Hatzigeorgiou, G. D. (2022). Shape correction factors for impact-echo method on short cylinders-A numerical and experimental study. 13th HSTAM International Congress on Mechanics (24-27 August), Patras, Greece.

[29] Wang, J. J., Chang, T. P., Chen, B. T., & Wang, H. (2012). Determination of Poissons ratio of solid circular rods by impact-echo method. Journal of Sound and Vibration, 331(5), 1059–1067. doi:10.1016/j.jsv.2011.10.030.

[30] Pelekis P., Siorikis, V. G., Antonopoulos, C. P., Hatzigeorgiou, G. D. (2022). Determination of Dynamic Elastic Properties on Short Cylinders Using Impact-Echo Method-A Numerical Study. 13th HSTAM International Congress on Mechanics (24-27 August), Patras, Greece.

[31] Greek Ministry of Environment Physical Planning and Public Works. (1997). Assessment of concrete's strength classification of existing structures. Accessed. Available online: http://fakisc.weebly.com/uploads/3/2/7/6/3276490/Εγκύκλιος_7_28-3-1997.pdf (accessed on August 2024).